VIP Oxidation States Very Important Paper

How to cite: *Angew. Chem. Int. Ed.* **2022,** *61,* e202207688
International Edition: doi.org/10.1002/anie.202207688
German Edition: doi.org/10.1002/ange.202207688

The Highest Oxidation State of Rhodium: Rhodium(VII) in $[RhO_3]^+$

Mayara da Silva Santos, Tony Stüker, Max Flach, Olesya S. Ablyasova, Martin Timm, Bernd von Issendorff, Konstantin Hirsch, Vicente Zamudio-Bayer, Sebastian Riedel,* and J. Tobias Lau**

Abstract: Although the highest possible oxidation states of all transition elements are rare, they are not only of fundamental interest but also relevant as potentially strong oxidizing agents. In general, the highest oxidation states are found in the electron-rich late transition elements of groups 7–9 of the periodic table. Rhodium is the first element of the 4d transition metal series for which the highest known oxidation state does not equal its group number of 9, but reaches only a significantly lower value of +6 in exceptional cases. Higher oxidation states of rhodium have remained elusive so far. In a combined mass spectrometry, X-ray absorption spectroscopy, and quantum-chemical study of gas-phase $[RhO_n]^+$ (n=1–4), we identify $[RhO_3]^+$ as the $^1A_1'$ trioxidorhodium(VII) cation, the first chemical species to contain rhodium in the +7 oxidation state, which is the third-highest oxidation state experimentally verified among all elements in the periodic table.

The formal concept of oxidation states is of fundamental importance in chemistry to characterize properties of elements in compounds.[1,2] The search for compounds with transition metals in their highest oxidation states[1,3–6] is not only of academic interest, but complexes with metal centers in unusually high oxidation states are of particular relevance in the context of strong oxidants[7–9] or fluorinating agents,[10–13] in catalytic processes,[14–19] and as intermediates in key reactions.[20,21]

Of the 4*d* transition elements, ruthenium, in the form of tetraoxido ruthenium(VIII),[22] is the last element for which the highest experimentally verified oxidation state corresponds to its group number. The highest known oxidation state for the next element in this series, rhodium, is +6 as has been proven for rhodium(VI) hexafluoride and a few other compounds.[23] In contrast, the highest oxidation states of its heavier 5d congener, iridium, agrees with its group number, and the tetraoxido iridium(IX) cation, $[IrO_4]^+$, represents the only known species with an element in oxidation state +9.[24] An even higher oxidation state has been claimed for group 10 with platinum(X) in $[PtO_4]^{2+}$,[6] although such species have not been verified experimentally so far, in line with the prediction that the dicationic species would decay into $[PtO_2]^+$.[5] Among the tetraoxido cations, the stability of group 9 elements in high oxidation states is compromised for the lighter congeners, cobalt and rhodium, because of the decreasing number of radial nodes in the 4d and 3d orbitals, which leads to less effective overlap with ligand orbitals.[1,4] Such behavior is assigned mainly to Pauli repulsion between ligand-based orbitals as the contraction of the metal *d* orbitals increases for higher oxidation states.[1,4] While nonavalent rhodium has been predicted in $[RhO_4]^+$ and $RhNO_3$, it has also been pointed out that highly covalent bonds in these species might lead to reconfiguration into isomers with rhodium in a lower oxidation state,[25] or even to the decay of $[RhO_4]^+$ by oxygen elimination.[26] Consequently, experimental and theoretical investigations show that rhodium forms dioxido-superoxido $[(\eta^1-O_2)RhO_2]$ or dioxido-peroxido $[(\eta^2-O_2)RhO_2]$ species with oxidation states of +5 and +6 instead of the tetraoxido isomer, RhO_4,[27,28] but the formation of $[RhO_3]^+$, as a candidate for rhodium(VII), has not been investigated experimentally or computationally so far.

Here, we present a gas-phase mass spectrometry and X-ray absorption spectroscopy study, combined with quantum-chemical calculations, of $[RhO_n]^+$ (n=0–4) cations. The formal oxidation states of rhodium in $[RhO_n]^+$ (n=0–4) are identified by rhodium M_3 and oxygen K-edge X-ray absorption spectroscopy with local excitation at the rhodium center or at the oxygen ligands, respectively, giving independent access to the local, non-bonding 4d configuration of rhodium, and to the nature of the oxygen species. For $[RhO_3]^+$ we also compare the experimental data to the simulated oxygen K-edge spectrum of the lowest energy

[*] M. da Silva Santos, M. Flach, O. S. Ablyasova, Prof. Dr. B. von Issendorff, Prof.Dr. J. T. Lau
Physikalisches Institut, Albert-Ludwigs-Universität Freiburg
Hermann-Herder-Straße 3, 79104 Freiburg (Germany)
M. da Silva Santos, M. Flach, O. S. Ablyasova, M. Timm, Dr. K. Hirsch, Dr. V. Zamudio-Bayer, Prof.Dr. J. T. Lau
Abteilung für Hochempfindliche Röntgenspektroskopie, Helmholtz-Zentrum Berlin für Materialien und Energie
Albert-Einstein-Straße 15, 12489 Berlin (Germany)
E-mail: mayara.da_silva_santos@helmholtz-berlin.de
tobias.lau@helmholtz-berlin.de
Dr. T. Stüker, Prof. Dr. S. Riedel
Institut für Chemie und Biochemie–Anorganische Chemie, Freie Universität Berlin
Fabeckstraße 34/36, 14195 Berlin (Germany)
E-mail: s.riedel@fu-berlin.de

isomer. Our results identify $[RhO_3]^+$ as a trioxido rhodium-(VII) cation, the first chemical species containing rhodium in the formal +7 oxidation state.

The experiments were performed at the ion-trap end-station, located at beamline UE52-PGM of the BESSY II synchrotron radiation facility, and computations were carried out using density functional theory as well as multi-reference methods. The experimental setup is described elsewhere,[29] and details of the experimental and computational methods are given in the Supporting Information.

In Figure 1, the experimental X-ray absorption spectrum of $[RhO_3]^+$ at the oxygen K-edge is shown, which is characterized by two main lines at 528.2 and 530.8 eV. These main features agree well with the X-ray absorption spectrum simulated with time-dependent density functional theory methods (TD-DFT, see Supporting Information for details), also shown in Figure 1, of $[RhO_3]^+$ in the $^1A_1'$ electronic ground state in D_{3h} point group symmetry. The calculated full spectrum is shown in Figure S6, where we see a poorer agreement between experiment and theory for excitations of higher energy at the oxygen K-edge. This effect is expected for TD-DFT studies as a consequence of the approximations made.[30] In order to compare absolute energies with the experimental data, the calculated spectrum was shifted by +19.7 eV. The structure optimizations of $[RhO_3]^+$ converge to a trigonal planar structure of D_{3h} symmetry with bond lengths of 167–169 pm, see Table S6, which are comparable with the bond length expected for a rhodium–oxygen double bond based on additive covalent radii of 167 pm.[31]

Figure 2 shows a depiction of the $^1A_1'$ electronic ground state of $[RhO_3]^+$, where the valence electrons are paired in the non-bonding a_2'' and a_1' molecular orbitals, representing the oxygen-centered $2p_z$ and rhodium-centered $4d_{z^2}$ atomic orbitals, respectively. The two-electron occupation of the a_1' orbital, along with the low electron density at any other d-derived molecular orbitals, suggest rhodium has a local $4d^2$ electronic configuration, which is consistent with an oxidation state of +7. Both components of the twofold degenerate e'' orbital show out-of-plane interaction of the atomic

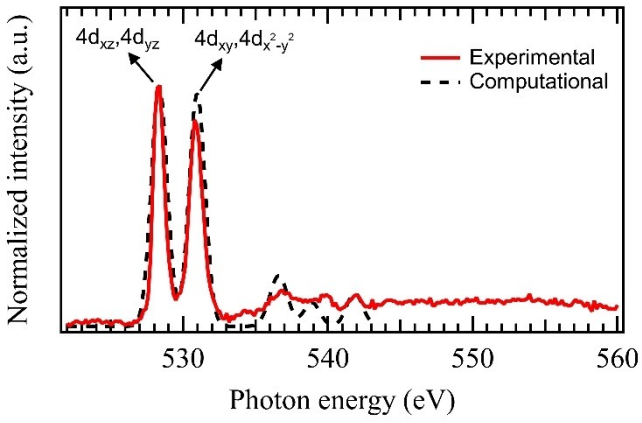

Figure 1. Experimental ion yield spectrum (solid red line) and computational TD-DFT X-ray absorption spectrum for the $^1A_1'$ ground state (dashed black line) of $[RhO_3]^+$, at the oxygen K-edge, with very good agreement for the transitions below 542 eV.

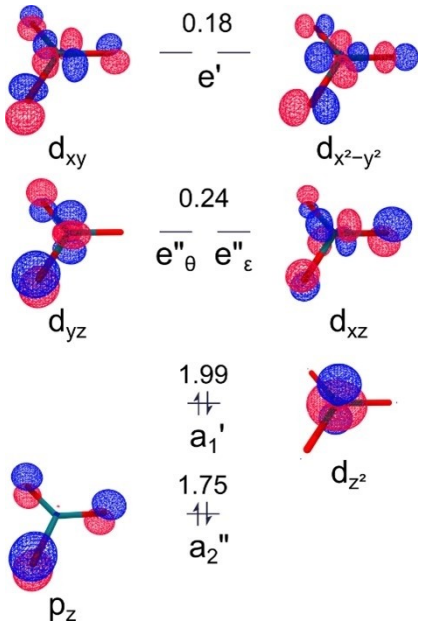

Figure 2. Frontier natural molecular orbital plot at 0.1 e Bohr^{-3} (state-specific CASSCF(15,20)/aug-cc-pVTZ-DK) for the $^1A_1'$ electronic ground state in D_{3h} point group symmetry of $[RhO_3]^+$ spanning the rhodium valence d orbital space, a_1', e'' and e', as well as the oxygen ligand centered a_1'' orbital. Arrows indicate the electron distribution of the leading configuration, while fractional numbers show the natural occupations. The fully (1.99 electrons) occupied, non-bonding a_1' ($4d^2$) orbital indicates rhodium in the formal +7 oxidation state.

orbitals along the bonds of anti-bonding π^* character, and are represented by e''_θ and e''_ϵ, for main rhodium atomic orbital contributions, d_{yz} and d_{xz}, respectively, while the components of the e' orbital show in-plane interactions, also of antibonding π^* character.

As indicated in Figure 1, the main features at the oxygen K-edge correspond to electronic excitations from the oxygen 1s orbital to the molecular e'' and e' orbitals, in which the main rhodium atomic orbital contributions are $4d_{xz}$ and $4d_{yz}$, for the 528.2 eV line, and $4d_{xy}$ and $4d_{x^2-y^2}$, for the 530.8 eV transition. This is in line with the very similar oxygen K-edge X-ray absorption spectrum of gas-phase $^1A_1'$ $[MnO_3]^+$, where two strong lines at 528.2 and 530.8 eV are also observed for the trioxido manganese(VII) cation.[32]

We have also investigated the lowest four excited states of $[RhO_3]^+$, see Supporting Information, the first two of which are triplet states, representing partial oxidations of the oxido ligands, and are energetically well separated from the electronic ground state by about 50 kJ mol^{-1}, see Table S2. The X-ray absorption spectrum at the oxygen K-edge was also calculated for these triplet states of $[RhO_3]^+$, but the band separations as well as the intensity ratios for the π^* transitions are not consistent with the experimental data, cf. Figure S6.

An overview of the oxygen K-edge spectra of the complete $[RhO_n]^+$ (n=0–4) series is shown in Figure 3. Here, the spectrum of $[RhO]^+$ can be taken as a reference for the oxido ligand signature in the predicted $^3\Sigma^-$ ground state[33,34] of $[RhO]^+$ with a bond dissociation energy of

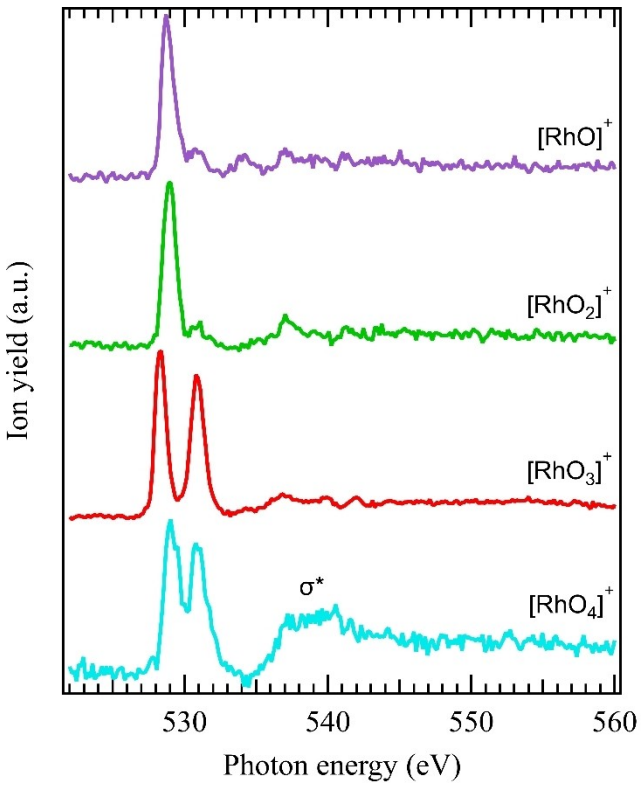

Figure 3. Ion yield spectra at the oxygen K edge of the $[RhO_n]^+$ ($n=0$–4) series. The absence of any oxygen-oxygen σ^* resonance for $n=1$–3 indicates purely oxido rhodium cations, while the presence of an oxygen-oxygen σ^* resonance for $[RhO_4]^+$ indicates the presence of at least one oxygen–oxygen bond.

3 eV.[35] The electronic configuration of $[RhO]^+$ suggests that the line observed at 528.72 eV corresponds to a transition into the oxygen $1s^{-1}6\pi^3$ excited state. Since the very similar spectrum of $[RhO_2]^+$ also indicates oxido ligands, in line with neutral $[RhO_2]$ species,[27] only oxido ligands are identified for the $[RhO_n]^+$ ($n=1$–3) series, and the formal oxidation states of rhodium can be assigned as +3, +5, and +7, respectively. In contrast, the $[RhO_4]^+$ species shows a σ^*-like transition around 540 eV, similar to the $1\sigma_g \rightarrow 3\sigma_u^*$ transition of molecular oxygen.[36,37] This σ^* resonance is an indication of the existence of an oxygen–oxygen bond, and is a characteristic spectroscopic fingerprint of chemisorbed or physisorbed dioxygen at metal surfaces in the peroxide or superoxide forms,[38,39] of solid-phase superoxides,[40,41] and of peroxide units in H_2O_2 and organic compounds.[42,43] This suggests the presence of at least one dioxygen unit in $[RhO_4]^+$, and thus confirms that tetraoxido rhodium is not formed.[25,27,28] Although the oxidation state of rhodium in $[RhO_4]^+$ cannot be unambiguously assigned from the oxygen K-edge alone, we tentatively assign the formal oxidation states of +4 or +5, see Supporting Information for details.

To further corroborate the unusual +7 oxidation state of rhodium, we have determined the oxidation state of the rhodium center in $[RhO_n]^+$ by evaluating chemical shifts of the rhodium M_3 excitation. This is a standard technique for 3d transition metals, which show a linear blueshift at the L edge as the oxidation state of the metal increases.[30,44] A similar chemical shift has also been observed for 4d transition metals, where the M_3 edge of molybdenum shows a shift of 0.49 eV per unit of oxidation state.[45]

Rhodium M_3-edge X-ray absorption spectra were measured for $[RhO_n]^+$ ($n=0$–4), see Supporting Information. The median M_3 excitation energy, calculated from the integrated intensity of the $[RhO_n]^+$ ($n=0$–4) spectra, cf. Table 1, indeed shows a systematic blueshift when plotted as a function of the formal oxidation state of the rhodium center in each species, cf. Figure 4, where $[RhO_4]^+$ is omitted because the oxidation state was not determined unambiguously. This correlation can be fitted linearly as $E_{M_3} = a + b \cdot OS_{Rh}$, where E_{M_3} is the median of the rhodium M_3 excitation energy, OS_{Rh} is the formal oxidation state of the rhodium atom, with coefficients $a=493.85\pm0.19$ eV and $b=0.88\pm0.04$ eV. In Table 1 and Figure 4 we have also included the formal occupation numbers of the non-bonding rhodium 4d derived valence orbitals, which are related to the rhodium M_3-edge shift and oxidation states,[2,44] for the rhodium cation and oxido rhodium cation series. We observe a chemical shift of the median M_3-edge excitation energy of

Table 1: Median values of the M_3-edge excitation energy, formal oxidation state (OS) of the rhodium atom and formal occupation of the rhodium-derived 4d valence orbitals for rhodium cation and $[RhO_n]^+$ ($n=1$–3) oxido species.

	Formal OS of Rh	Rh(4d) formal occupation	Median [eV]
Rh^+	+1	$4d^8$	494.67±0.15
$[RhO]^+$	+3	$4d^6$	496.48±0.15
$[RhO_2]^+$	+5	$4d^4$	498.49±0.15
$[RhO_3]^+$	+7	$4d^2$	499.90±0.15

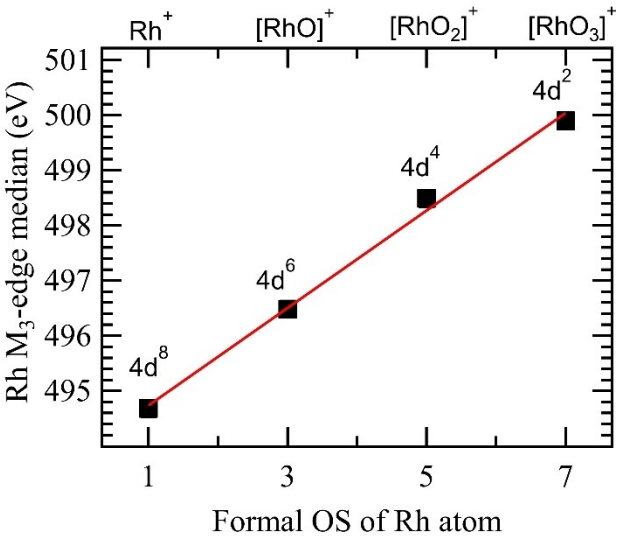

Figure 4. Median values, calculated from the integrated intensity of the rhodium M_3 edge of $[RhO_n]^+$ ($n=0$–3) species, plotted as a function of the formal oxidation state of the rhodium center, with a linear fit shown as a red line. The formal occupation of the (non-bonding) rhodium 4d atomic orbitals is indicated in the figure. Cf. Table 1 for numerical values.

0.88 ± 0.04 eV per unit of oxidation state, which is comparable to the chemical shift of 0.82 eV observed at the L_3-edge of iron[46] and, in general, is between the values found for the molybdenum M_3-edge, of 0.49 eV,[45] and for the L_3-edge of 3d transition metals, of 1–2 eV.[46,47] The observed linear dependence of M_3 shift and rhodium oxidation state is a confirmation of the assigned +7 oxidation state in $[RhO_3]^+$, in full agreement with our theoretical results and with the identification of a trioxido species from oxygen K-edge X-ray absorption spectroscopy.

In summary, we have characterized the highest oxidation state of rhodium observed so far, rhodium(VII) in $[RhO_3]^+$, by combination of mass spectrometry, X-ray absorption spectroscopy, and quantum-chemical calculations. This makes rhodium the third 4d transition element to form the rare formal +7 oxidation state, along with technetium and ruthenium. Because of its unusually high oxidation state, $[RhO_3]^+$ should be a strong oxidizing agent, and we would expect gas-phase reactivity studies[48] to reflect on this behavior. Our predicted vertical electron affinity of $[RhO_3]^+$, which is 10.6 eV and 11.1 eV at the CCSD(T) and B3LYP levels, respectively, is higher than 9.59 eV[49,50] for NO_2^+ but significantly lower than 12.07 eV[51] for O_2^+. Since O_2^+ is stabilized by weakly coordinating anions like $[PtF_6]^-$, $[BF_4]^-$, or $[AsF_6]^-$, it might be possible to also stabilize $[RhO_3]^+$, based on its electron affinity as shown, e.g., for the stabilization of $[IrO_4]^+$.[26]

Acknowledgements

Beamtime for this project was granted at the Ion Trap endstation of BESSY II, beamline UE52-PGM, operated by Helmholtz-Zentrum Berlin. This project has received funding from the German Federal Ministry of Education and Research through Grant No. BMBF-05K16VF1. BvI, JTL, MF, and OA acknowledge support by DFG RTG 2717. SR and TS acknowledge funding by ERC Project HighPotOx (818862). Computing time was made available by the High-Performance Computing Center at ZEDAT, Freie Universität Berlin. Open Access funding enabled and organized by Projekt DEAL.

Conflict of Interest

The authors declare no conflict of interest.

Data Availability Statement

The data that support the findings of this study are available from the corresponding author upon reasonable request.

Keywords: Gas Phase · Oxidation State · Oxides · Rhodium · X-Ray Absorption Spectroscopy

[1] S. Riedel, M. Kaupp, *Coord. Chem. Rev.* **2009**, *253*, 606–624.
[2] C. K. Jørgensen, *Oxidation Numbers and Oxidation States*, Springer Berlin Heidelberg, Berlin, **1969**.
[3] C. K. Jørgensen, *Naturwissenschaften* **1976**, *63*, 292–292.
[4] T. Schlöder, S. Riedel, *Comprehensive Inorganic Chemistry II*, Elsevier, Amsterdam, **2013**, pp. 227–243.
[5] S.-X. Hu, W.-L. Li, J.-B. Lu, J. L. Bao, H. S. Yu, D. G. Truhlar, J. K. Gibson, J. Marçalo, M. Zhou, S. Riedel, W. H. E. Schwarz, J. Li, *Angew. Chem. Int. Ed.* **2018**, *57*, 3242–3245; *Angew. Chem.* **2018**, *130*, 3297–3300.
[6] H. S. Yu, D. G. Truhlar, *Angew. Chem. Int. Ed.* **2016**, *55*, 9004–9006; *Angew. Chem.* **2016**, *128*, 9150–9152.
[7] W. Levason, F. M. Monzittu, G. Reid, W. Zhang, E. G. Hope, *J. Fluorine Chem.* **2017**, *200*, 190–197.
[8] B. C. Bales, P. Brown, A. Dehestani, J. M. Mayer, *J. Am. Chem. Soc.* **2005**, *127*, 2832–2833.
[9] G. Green, W. P. Griffith, D. M. Hollinshead, S. V. Ley, M. Schröder, *J. Chem. Soc. Perkin Trans. 1* **1984**, 681–686.
[10] N. Bartlett, *Angew. Chem. Int. Ed. Engl.* **1968**, *7*, 433–439; *Angew. Chem.* **1968**, *80*, 453–460.
[11] J. H. Holloway, E. G. Hope, P. J. Townson, R. L. Powell, *J. Fluorine Chem.* **1996**, *76*, 105–107.
[12] W. W. Dukat, J. H. Holloway, E. G. Hope, M. R. Rieland, P. J. Townson, R. L. Powell, *J. Chem. Soc. Chem. Commun.* **1993**, 1429–1430.
[13] J. Lin, S. Zhang, W. Guan, G. Yang, Y. Ma, *J. Am. Chem. Soc.* **2018**, *140*, 9545–9550.
[14] J. H. Canterford, T. A. O'Donnell, *Aust. J. Chem.* **1968**, *21*, 1421–1425.
[15] F. Tamadon, S. Seidel, K. Seppelt, *Acta Chim. Slov.* **2013**, *60*, 491–494.
[16] W. Levason, F. M. Monzittu, G. Reid, *Coord. Chem. Rev.* **2019**, *391*, 90–130.
[17] W. Levason, F. M. Monzittu, G. Reid, W. Zhang, *Chem. Commun.* **2018**, *54*, 11681–11684.
[18] K. Seppelt, *Chem. Rev.* **2015**, *115*, 1296–1306.
[19] W. P. Griffith, S. V. Ley, G. P. Whitcombe, A. D. White, *J. Chem. Soc. Chem. Commun.* **1987**, 1625–1627.
[20] V. Piccialli, *Synthesis* **2007**, 2585–2607.
[21] T. A. Betley, Q. Wu, T. Van Voorhis, D. G. Nocera, *Inorg. Chem.* **2008**, *47*, 1849–1861.
[22] C. Claus, *J. Prakt. Chem.* **1860**, *79*, 28–59.
[23] C. L. Chernick, H. H. Claassen, B. Weinstock, *J. Am. Chem. Soc.* **1961**, *83*, 3165–3166.
[24] G. Wang, M. Zhou, J. T. Goettel, G. J. Schrobilgen, J. Su, J. Li, T. Schlöder, S. Riedel, *Nature* **2014**, *514*, 475–477.
[25] M. A. Domański, Ł. Wolański, P. Szarek, W. Grochala, *J. Mol. Model.* **2020**, *26*, 52.
[26] D. Himmel, C. Knapp, M. Patzschke, S. Riedel, *ChemPhysChem* **2010**, *11*, 865–869.
[27] A. Citra, L. Andrews, *J. Phys. Chem. A* **1999**, *103*, 4845–4854.
[28] Y. Gong, M. Zhou, L. Andrews, T. Schlöder, S. Riedel, *Theor. Chem. Acc.* **2011**, *129*, 667–676.
[29] K. Hirsch, J. T. Lau, P. Klar, A. Langenberg, J. Probst, J. Rittmann, M. Vogel, V. Zamudio-Bayer, T. Möller, B. von Issendorff, *J. Phys. B* **2009**, *42*, 154029.
[30] F. Frati, M. O. J. Y. Hunault, F. M. F. De Groot, *Chem. Rev.* **2020**, *120*, 4056–4110.
[31] P. Pyykkö, M. Atsumi, *Chem. Eur. J.* **2009**, *15*, 12770–12779.
[32] M. G. Delcey, R. Lindblad, M. Timm, C. Bülow, V. Zamudio-Bayer, B. von Issendorff, J. T. Lau, M. Lundberg, *Phys. Chem. Chem. Phys.* **2022**, *24*, 3598–3610.
[33] P. Song, W. Guan, C. Yao, Z. M. Su, Z. J. Wu, J. D. Feng, L. K. Yan, *Theor. Chem. Acc.* **2007**, *117*, 407–415.
[34] I. R. Ariyarathna, N. M. S. Almeida, E. Miliordos, *Phys. Chem. Chem. Phys.* **2020**, *22*, 16072–16079.

[35] Y. Chen, P. B. Armentrout, *J. Chem. Phys.* **1995**, *103*, 618–625.
[36] Y. Meng, P. J. Eng, J. S. Tse, D. M. Shaw, M. Y. Hu, J. Shu, S. A. Gramsch, C.-C. Kao, R. J. Hemley, H.-K. Mao, *Proc. Natl. Acad. Sci. USA* **2008**, *105*, 11640–11644.
[37] J. Stöhr, *NEXAFS Spectroscopy*, Springer Berlin Heidelberg, Berlin, **1992**, pp. 79–113.
[38] D. A. Outka, J. Stöhr, W. Jark, P. Stevens, J. Solomon, R. J. Madix, *Phys. Rev. B* **1987**, *35*, 4119–4122.
[39] W. Wurth, J. Stöhr, P. Feulner, X. Pan, K. R. Bauchspiess, Y. Baba, E. Hudel, G. Rocker, D. Menzel, *Phys. Rev. Lett.* **1990**, *65*, 2426–2429.
[40] J.-S. Kang, D. H. Kim, J. H. Hwang, J. Baik, H. J. Shin, M. Kim, Y. H. Jeong, B. I. Min, *Phys. Rev. B* **2010**, *82*, 193102.
[41] M. W. Ruckman, J. Chen, S. L. Qiu, P. Kuiper, M. Strongin, B. I. Dunlap, *Phys. Rev. Lett.* **1991**, *67*, 2533–2536.
[42] E. Rühl, A. P. Hitchcock, *Chem. Phys.* **1991**, *154*, 323–329.
[43] K. L. Harding, S. Kalirai, R. Hayes, V. Ju, G. Cooper, A. P. Hitchcock, M. R. Thompson, *Chem. Phys.* **2015**, *461*, 117–124.
[44] G. Van Der Laan, I. W. Kirkman, *J. Phys. Condens. Matter* **1992**, *4*, 4189–4204.
[45] J. Chen, *Catal. Today* **1998**, *43*, 147–158.
[46] H. Tan, J. Verbeeck, A. Abakumov, G. Van Tendeloo, *Ultramicroscopy* **2012**, *116*, 24–33.
[47] J. K. Kowalska, B. Nayyar, J. A. Rees, C. E. Schiewer, S. C. Lee, J. A. Kovacs, F. Meyer, T. Weyhermüller, E. Otero, S. Debeer, *Inorg. Chem.* **2017**, *56*, 8147–8158.
[48] D. Schröder, H. Schwarz, S. Shaik, *Metal-Oxo and Metal-Peroxo Species in Catalytic Oxidations*, Springer Berlin Heidelberg, Berlin, **2007**, pp. 91–123.
[49] K. S. Haber, J. W. Zwanziger, F. X. Campos, R. T. Wiedmann, E. R. Grant, *Chem. Phys. Lett.* **1988**, *144*, 58–64.
[50] D. E. Clemmer, P. B. Armentrout, *J. Chem. Phys.* **1992**, *97*, 2451–2458.
[51] R. G. Tonkyn, J. W. Winniczek, M. G. White, *Chem. Phys. Lett.* **1989**, *164*, 137–142.

Manuscript received: May 25, 2022
Accepted manuscript online: July 12, 2022
Version of record online: August 10, 2022